Theory of ferroelectric phase transition of polymers

Susumu Ikeda and Hiroyuki Suda
Department of Materials Science and Engineering, Faculty of Engineering, Yamagata University, Jonan 4-3-16, Yonezawa 992, Japan
(Received 4 September 1996)

We propose a model of ferroelectric polymers constructed through abstraction of ferroelectric properties of copolymers of vinylidene fluoride and trifluoroethylene. Each element in the model can take two different structures whose energy states are split into three levels under an electric field. Interaction between elements in this system is classified into two categories; intermolecular interaction and intramolecular interaction. Fundamental properties of the model are calculated by the Bethe approximation. We find the thermodynamic character of the phase transition changes from the first order phase transition to the diffuse transition with a change in the ratio of intermolecular and intramolecular interactions. We demonstrate a critical phenomenon at a boundary between the first order phase transition and the diffuse transition. The critical temperature is independent of the properties related to the intramolecular degrees of freedom such as intramolecular interaction and multiplicity of an excited conformation state. Furthermore, a smearing out effect that is introduced into the intermolecular interaction influences the transition temperature. The effects of external fields on the phase transition are also discussed. [S1063-651X(97)03509-5]

PACS number(s): 05.70.Jk, 64.60.Cn, 77.84.Jd, 77.80.−e

I. INTRODUCTION

The crystal of fluorocopolymers including vinylidene fluoride (VDF) exhibits ferroelectric properties below a phase transition temperature T_t and loses them above T_t [1–6]. Then, values characterizing the phase transition such as the transition temperature and temperature hysteresis, which is defined as the temperature difference between the transition temperatures during heating and during cooling, vary as a function of a VDF ratio in the copolymer. Such phenomena have been observed particularly for copolymers of VDF and trifluoroethylene (TrFE) using various experimental methods [3,7]. It has been shown experimentally in the copolymer that the thermodynamic character of the phase transition is changed from a first order phase transition to a diffuse transition through the second order phase transition by a decrease in the VDF ratio [8,9].

This phase transition has been categorized as being an order-disorder type phase transition [4]. In the ferroelectric phase, the polarization made of oriented permanent dipoles belonging to VDF monomers is cooperatively reversed by an external electric field [10]. Such the order-disorder-type phase transition and the cooperative polarization reversal are mainly controlled by the intermolecular interaction. In this case, furthermore, when the ferroelectric phase is transformed into the paraelectric one, gauche bonds mix to a chain composed of all trans bonds. Then an intramolecular interaction plays an important role in the ferroelectric phase transition [11–16].

The short range interaction working between atoms is classified into two sorts: the intermolecular interaction works between two atoms belonging to different molecules and the intramolecular interaction works between two atoms belonging to the same molecule and existing always within an interaction range of each other. The role of these interactions for selection of molecular conformation and crystal structure was discussed in the case of polyvinylidene fluoride (PVDF) [17]. It was found that a PVDF chain prefers a chain conformation including a gauche bond to a conformation consisting of all trans bonds because of an advantage of the intramolecular interaction. The advantage of the gauche bond in the intramolecular interaction, however, decreases with the increase of molecular defects such as head-to-head linkages. Since the introduction of TrFE to a VDF chain is considered to be the same as the introduction of defects, increasing the TrFE ratio makes the trans bond more stable in a point of the intramolecular interaction. The characteristic of a VDF-TrFE copolymer varying with the copolymerization ratio is considered to come from the property of this intramolecular interaction.

The purposes of this paper are to abstract the ferroelectric phase transition of VDF-TrFE copolymers, to construct a model, and to give a natural figure of the model. Furthermore, the effects of the several external fields on the system are discussed.

II. ABSTRACTION OF PHENOMENA

The interaction governing the behavior of atoms in a polymer crystal has remarkable anisotropy. Positional relations between neighboring atoms within a molecule are governed by a covalent bond. The atoms that are not bonded by the covalent bond combine with one another by a secondary interaction such as the van der Waals interaction. Since the covalent bond force is much stronger than the other force, conformations of a polymer chain change within a restriction placed by the covalent bond. In an amorphous region where the intermolecular interaction is rather weak, either trans conformation or gauche transformation is selected by the secondary force working dominantly between two carbons at a distance of three covalent bonds away from each other. When the difference due to the intermolecular interaction is neglected, we call the energy difference between the trans conformation and gauche one the intramolecular interaction energy. In many polymers, the trans sequence leads to a pla-

nar zigzag conformation and mixing of gauche bonds to a helical one.

It is well known as a result of experimental studies that copolymers including vinylidene fluoride take a planar zigzag conformation consisting of all trans sequences in the ferroelectric state but, on the other hand, they take a sort of helical conformation including randomly gauche bonds in the paraelectric state [3]. The copolymer chain has the maximum dipole moment in the planar zigzag conformation and loses the dipole moment in the helical conformation. The spontaneous polarization of the system is formed by parallel orientation of the dipoles of planar zigzag chains.

It is expected that the ferroelectric ground state that is composed of parallel alignment of dipoles belonging to planar zigzag chain segments is excited through two different processes. One is an intermolecularly mixing process of antiparallel dipoles, both of which are held by trans bond sequences. In this case the planar zigzag conformation of the chains is unchanged. This mode of excitation is the same as that in the Ising model. The other process is an intramolecularly mixing process of gauche and trans bonds. In this case, the planar zigzag conformation is transformed to a random helix whose net dipole moment becomes zero. The spontaneous polarization of the ferroelectric state, thus, decreases gradually toward zero in the paraelectric state.

The intramolecular interaction selects the gauche bond rather than the trans one in a range of VDF ratio higher than about 65 mol % [3]. Even in such a case, molecular chains in the ferroelectric state are in a planar zigzag conformation made of only the trans bond. The reason is that an intermolecularly parallel packing of the planar zigzag molecules is preferred to an antiparallel one or the other packing way including a helical chain by the intermolecular interaction. Consequently, in the ferroelectric state, dipoles of molecules line up parallel with each other. Such a situation suggests that a main driving force that causes this polymer to be ferroelectric is an intermolecular force working between molecular chains.

A force originating from an intramolecular interaction also affects ferroelectric properties of the polymer. It works drastically on the conformational change occurring when the ferroelectric phase transition takes place.

An electric dipole-dipole interaction with a long interaction range is neglected because it is known as a result of a theoretical study on PVDF that the interaction is ineffective in PVDF [18,19].

III. MODEL

An element in our model can take three states. Two states g and e, which denote ''ground'' and ''excited,'' can be distinguished morphologically; g corresponds to a planar zigzag conformation consisting of all trans bonds and e a random helix including randomly gauche bonds. Furthermore, g is split by an electric field into two energy states g_1 and g_{-1} with dipoles μ and $-\mu$, respectively, and the other state e has no dipole moment.

Considering anisotropic mechanical properties of polymers, we construct a two-dimensional model on a cross section perpendicular to a molecular axis. So we can symbolize the three states as an up-directed arrow, a down-directed arrow, and a circle as shown in Fig. 1.

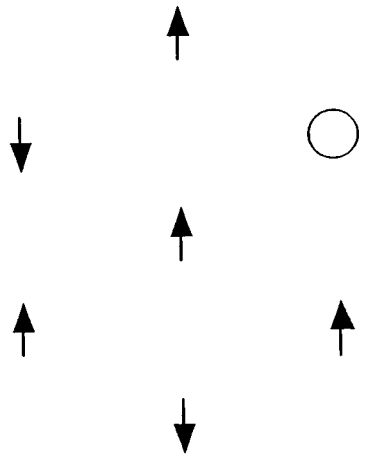

FIG. 1. Cross section of ferroelectric polymer model packed hexagonally.

In such a system, the ferroelectric phase is realized by cooperative organization into the state g_1 or g_{-1}. On the other hand, the paraelectric phase is made of elements of the state e and domains including equally g_1 and g_{-1}. The ferroelectric phase transition of this system, therefore, means a transformation of an ordered state of g_1 or g_{-1} into the e state or into a disordered mixture of g_1 and g_{-1}.

The interaction is categorized to intermolecular and intramolecular interactions. Intermolecular interaction is considered between the segments belonging to different molecular chains, therefore, between the elements in this model. Since the intramolecular interaction is taken as the energy difference between a trans and a gauche bond, we assigned it to the energy difference between g and e in this model.

The intramolecular interaction characteristic of each conformation of the element and the intermolecular interaction characteristic of each couple of elements are listed in Table I. The intermolecular interaction is measured as the difference from the intermolecular interaction energy of the standard couple including the excited element e. The parallel and antiparallel couples between elements in the g state are assumed to be placed energetically below and above the standard couple, respectively, and at an equal distance from it.

In this table, the Boltzmann factor for the e state is mul-

TABLE I. Potential parameters and Boltzmann factors.

1. Intermolecular interaction between center site and nearest neighbors

Couples	Potential	Boltzmann factor
g_1-g_1, $g_{-1}-g_{-1}$	$-V$	$X=\exp(V/kT)$
$e-g$, $e-e$	0	1
g_1-g_{-1}	V	$1/X$

2. Intramolecular interaction

Conformation	Potential	Boltzmann factor
e	W	$Y=A\ \exp(-W/kT)$
g	0	1

tiplied by A. This means there are several ways to place an element of the e state on the two-dimensional lattice, although there is only one way for g_1 and g_{-1}.

IV. THEORY

A. Molecular field approximation

We first treat the system with a molecular field approximation. The Hamiltonian of the system is described as

$$H=-V\sum_{i>j}\sigma_i\sigma_j+W\sum_i(1-\sigma_i^2). \tag{1}$$

Here σ take values -1, 0, and 1, which stand for g_{-1}, e, and g_1, respectively. The first term represents an intermolecular interaction and the second term an intramolecular one. Since ferroelectricity is treated here, V is positive. From the first term of Eq. (1) we can find that if dipoles are lined up parallel with each other, the system is stabilized in comparison with the antiparallel configuration. The second term vanishes when $|\sigma|$ is 1, which means that gauche bonds are not included. That is, if the gauche conformation is preferred to the trans one by the intramolecular interaction, W has a negative value. On the other hand, the positive W selects the trans conformation. When an average $\langle\sigma\rangle$ is substituted for σ_j, the interaction energy for the element at the site i, $H(i)$, may be described as

$$H(i)=-zV\langle\sigma\rangle\sigma_i+W(1-\sigma_i^2). \tag{2}$$

Here z is a coordination number of the site. The statistical average of σ is described as

$$\langle\sigma\rangle=\frac{\sum_{\sigma_i=-1}^{1}\sigma_i\xi(\sigma_i)\exp[-\beta H(i)]}{Z_1}. \tag{3}$$

Here, $W=nV$ and Z_1 is a one-particle partition function. Furthermore, the degeneracy parameter $\xi(\sigma_i)$ is set as $\xi(1)=\xi(-1)=1$ and $\xi(0)=A$ as described in the previous section. Setting as $kT/V=T^*$ and $\beta nV=n/T^*$, Eq. (3) is rewritten as

$$\langle\sigma\rangle=\frac{2\sinh[\langle\sigma\rangle/T^*]}{2\cosh[\langle\sigma\rangle/T^*]+A\exp[-(n/T^*)]}. \tag{4}$$

As inferred easily from the model, this solution is that of a two-dimensional Ising model if the second term in the denominator vanishes. This premise means that the gauche conformation cannot be realized because of a high intramolecular potential barrier.

B. Bethe approximation

The model described above is treated in terms of the Bethe approximation. The treated system is composed of 7 elements, which include the center element and the surrounding 6 elements. The partial partition function can be given by the following procedure. If the center site is occupied by the g_1 element and 6 surrounding sites are also occupied by a g_1 elements, b g_{-1} elements, and c e elements, then the contribution of the configuration to the partition function becomes

$${}_6C_a(XM)^a{}_{6-a}C_b(XM)^{-b}Y^c. \tag{5}$$

Here, M represents the contribution of a molecular field coming from the sites surrounding the nearest sites and will be described in Eq. (13). The results given by the same procedure are summarized in Table II for all cases of combinations of elements in the model system.

TABLE II. Boltzmann factor for each configuration of model system.

Nearest neighbor	Center g_1	Site g_{-1}	e
$6g_1$	X^6M^6	$X^{-6}M^6$	M^6Y
$5g_1,g_{-1}$	$6X^4M^4$	$6X^{-4}M^4$	$6M^4Y$
$4g_1,2g_{-1}$	$15X^2M^2$	$15X^{-2}M^2$	$15M^2Y$
$3g_1,3g_{-1}$	20	20	$20Y$
$2g_1,4g_{-1}$	$15X^{-2}M^{-2}$	$15X^2M^{-2}$	$15M^{-2}Y$
$g_1,5g_{-1}$	$6X^{-4}M^{-4}$	$6X^4M^{-4}$	$6M^{-4}Y$
$6g_{-1}$	$X^{-6}M^{-6}$	X^6M^{-6}	$M^{-6}Y$
$5g_1,e$	$6X^5M^5Y$	$6X^{-5}M^5Y$	$6M^5Y^2$
$4g_1,2e$	$15X^4M^4Y^2$	$15X^{-4}M^4Y^2$	$15M^4Y^3$
$3g_1,3e$	$20X^3M^3Y^3$	$20X^{-3}M^3Y^3$	$20M^3Y^4$
$2g_1,4e$	$15X^2M^2Y^4$	$15X^{-2}M^2Y^4$	$15M^2Y^5$
$g_1,5e$	$6XMY^5$	$6X^{-1}MY^5$	$6MY^6$
$6e$	Y^6	Y^6	Y^7
$4g_1,g_{-1},e$	$30X^3M^3Y$	$30X^{-3}M^3Y$	$30M^3Y^2$
$3g_1,g_{-1},2e$	$60X^2M^2Y^2$	$60X^{-2}M^2Y^2$	$60M^2Y^3$
$2g_1,g_{-1},3e$	$60XMY^3$	$60X^{-1}MY^3$	$60MY^4$
$g_1,g_{-1},4e$	$30Y^4$	$30Y^4$	$30Y^5$
$g_{-1},5e$	$6X^{-1}M^{-1}Y^5$	$6XM^{-1}Y^5$	$6M^{-1}Y^6$
$3g_1,2g_{-1},e$	$60XMY$	$60X^{-1}MY$	$60MY^2$
$2g_1,2g_{-1},2e$	$90Y^2$	$90Y^2$	$90Y^3$
$g_1,2g_{-1},3e$	$60X^{-1}M^{-1}Y^3$	$60XM^{-1}Y^3$	$60M^{-1}Y^4$
$2g_{-1},4e$	$15X^{-2}M^{-2}Y^4$	$15X^2M^{-2}Y^4$	$15M^{-2}Y^5$
$2g_1,3g_{-1},e$	$60X^{-1}M^{-1}Y$	$60XM^{-1}Y$	$60M^{-1}Y^2$
$g_1,3g_{-1},2e$	$60X^{-2}M^{-2}Y^2$	$60X^2M^{-2}Y^2$	$60M^{-2}Y^3$
$3g_{-1},3e$	$20X^{-3}M^{-3}Y^3$	$20X^3M^{-3}Y^3$	$20M^{-3}Y^4$
$g_1,4g_{-1},e$	$30X^{-3}M^{-3}Y$	$30X^3M^{-3}Y$	$30M^{-3}Y^2$
$4g_{-1},2e$	$15X^4M^{-4}Y^2$	$15X^4M^{-4}Y^2$	$15M^{-4}Y^3$
$5g_{-1},e$	$6X^{-5}M^{-5}Y$	$6X^5M^{-5}Y$	$6M^{-5}Y^2$

Summing up each column in Table II gives relative probabilities P_1', P_{-1}', and P_0', which stand for the probabilities of the configuration in which the center sites are filled with g_1, g_{-1}, and e, respectively.

$$P_1'=[XM+(XM)^{-1}+Y]^6, \tag{6}$$

$$P_{-1}'=[X/M+(X/M)^{-1}+Y]^6, \tag{7}$$

$$P_0'=Y[M+M^{-1}+Y]^6. \tag{8}$$

Here we estimate the molecular field M. The probability that the element at some site takes each state g_1, g_{-1}, or e is

TABLE III. Molecular field applied to nearest neighbors from surrounding sites.

Nearest site	Potential	Boltzmann factor
g_1	U	$M=\exp(-U/kT)$
e	0	1
g_{-1}	$-U$	$1/M$

described as follows in the molecular field approximation when Z is a partition function:

$$P_1/Z, \quad P_{-1}/Z, \quad P_0/Z, \tag{9}$$

$$Z=P_1+P_{-1}+P_0. \tag{10}$$

Here, 6 sites in the nearest neighbor sites interact with $6P_1$ pieces of g_1 elements, $6P_{-1}$ pieces of g_{-1} elements, and $6P_0$ pieces of e elements. When the nearest site is filled with g_1, the g_1 element is captured by the molecular field U, which is described as

$$U=6(P_1/Z)(-V)+6(P_{-1}/Z)V, \tag{11}$$

$$=-6P_SV, \tag{12}$$

where $P_S=(P_1-P_{-1})/Z$ means the normalized spontaneous polarization in this model. Therefore, the Boltzmann factor M can be written as

$$M=\exp(-U/kT)=X^{6P_S}. \tag{13}$$

The molecular field for the other case is given in Table III. We can rewrite Eqs. (6)–(8) using Table III as

$$P'_{-1}=(X^{-6P_S+1}+X^{6P_S-1}+Y)^6, \tag{14}$$

$$P'_1=(X^{6P_S+1}+X^{-6P_S-1}+Y)^6, \tag{15}$$

$$P'_0=(X^{6P_S}+X^{-6P_S}+Y)^6. \tag{16}$$

Using a similar procedure, on the other hand, we can also find the relative probabilities that one of 6 nearest neighbor sites is g_1, g_{-1}, or e. Abbreviating them as P''_1, P''_{-1}, and P''_0, we have

$$P''_1=X^{6P_S}[X(X^{6P_S+1}+X^{-6P_S-1}+Y)^5+X^{-1}(X^{-6P_S+1}+X^{6P_S-1}+Y)^5+Y(X^{6P_S}+X^{-6P_S}+Y)^5], \tag{17}$$

$$P''_{-1}=X^{-6P_S}[X^{-1}(X^{6P_S+1}+X^{-6P_S-1}+Y)^5+X(X^{-6P_S+1}+X^{6P_S-1}+Y)^5+Y(X^{6P_S}+X^{-6P_S}+Y)^5], \tag{18}$$

$$P''_0=Y[(X^{6P_S+1}+X^{-6P_S-1}+Y)^5+(X^{-6P_S+1}+X^{6P_S-1}+Y)^5+Y(X^{6P_S}+X^{-6P_S}+Y)^5]. \tag{19}$$

Self-consistency relations between the center site and nearest neighbor sites become

$$P'_1=P''_1, \quad P'_{-1}=P''_{-1}, \quad P'_0=P''_0. \tag{20}$$

These relations give the temperature dependence of the spontaneous polarization in the system where intermolecular and intramolecular interactions with various magnitudes act effectively.

V. NUMERICAL CALCULATION AND RESULTS

Figure 2 shows variations in transition curves represented as P_s vs T when $n\equiv W/V$ is taken as a variable parameter and $A=10$ as a constant. The temperature in an abscissa is normalized by the critical temperature T_{cI} of the Ising model corresponding to the case where n equals positive infinity. The transition temperature T_t increases with increasing n, which means W increases. When n has a negative value and W is negative, the transition becomes the first order phase transition, that exhibits the temperature hysteresis. In those curves, the highest temperature $T_{\rm th}$ in a temperature range where P_s is a three valued function may be identified with the transition temperature measured in a heating experiment. The lowest temperature in the same temperature range $T_{\rm tl}$ is also identified with the transition temperature measured in a

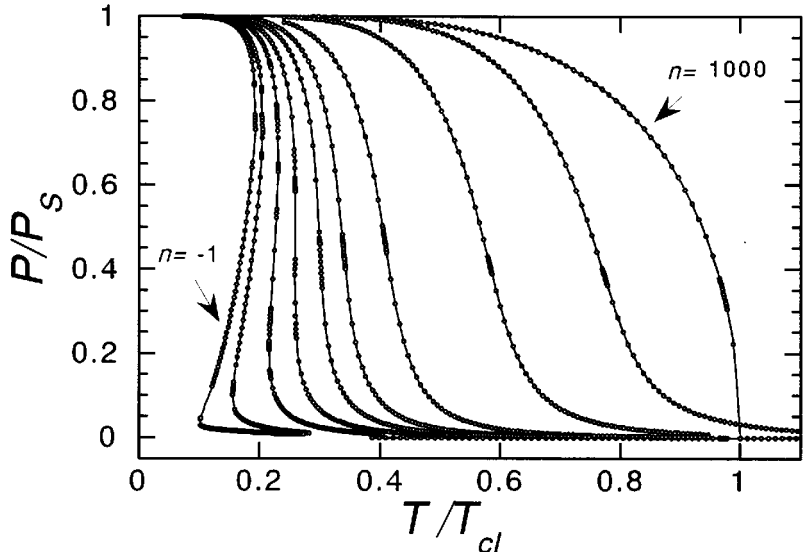

FIG. 2. Polarization vs temperature relations during the ferroelectric phase transition for the model with $A=10$. Critical temperature of the Ising model is described as T_{cI}. The transition changes from the diffuse transition to the first order phase transition through the second order phase transition with decreasing value of n. The values of n are 1000, 10, 5, 2, 1, 0.5, 0, -0.4, -0.8, and -1 from the right to the left.

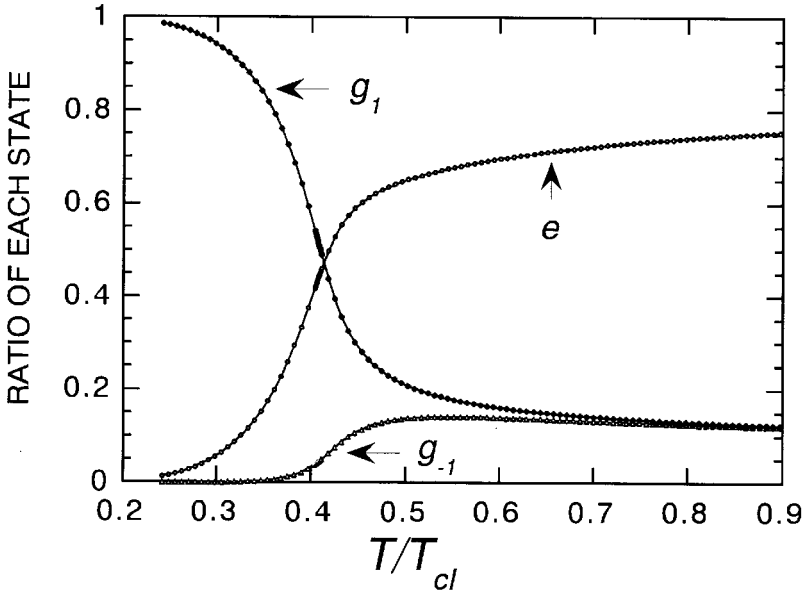

FIG. 3. Temperature dependence of the existence ratio of each state when n equals 5.

cooling experiment. We can estimate the temperature hysteresis observed in the first order phase transition as $\Delta T \equiv T_{\mathrm{th}} - T_{\mathrm{tl}}$. As n increases the character of the transition is transformed from the first order phase transition, which exhibits the clear temperature hysteresis, to a diffuse transition through the second order phase transition. The transition temperature T_t in the diffuse transitions is determined by taking the temperature where the transition curve exhibits the maximum slope. In the range of n where the diffuse transition is occurring, the transition curves approach again the second order phase transition with increasing n. It turns out that the model becomes the Ising system when n approaches positive infinity. This figure shows that the variation in the phase transition, from the the first order phase transition to the diffuse transition, which occurs far from the critical point of the Ising system, explains the dependence of the ferroelectric properties upon the VDF fraction included in VDF-TrFE copolymers.

Figures 3 and 4 illustrate what is occurring in the two curves shown in Fig. 2 corresponding to $n=5$ and -0.8. Figure 3 corresponding to $n=5$ represents the diffuse transition and Fig. 4 corresponding to $n=-0.8$ represents the first order phase transition. These figures illustrate the phase transition from the ordered state in g_1 to the disordered state distributed equally among g_1, g_{-1}, and e. The branch of the e state has an existence ratio of $\frac{5}{6}$ in the disordered state in high temperatures and those of g_1 and g_{-1} equal $\frac{1}{12}$. Above T_c the ratio of g increases or decreases according to negative or positive intramolecular interaction, respectively. It shows that thermal excitations are occurring across the intramolecular interaction when the intermolecular environment is averaged in the paraelectric state. This theoretical result agrees well with the experimental ones measured in IR experiments by Tashiro *et al.* [3].

Figures 5 and 6 show phase diagrams when A equals 10. When n becomes smaller than 20, the transition temperature is going down abruptly from T_{cI} of the Ising model. This means that the existence of an excited conformation begins

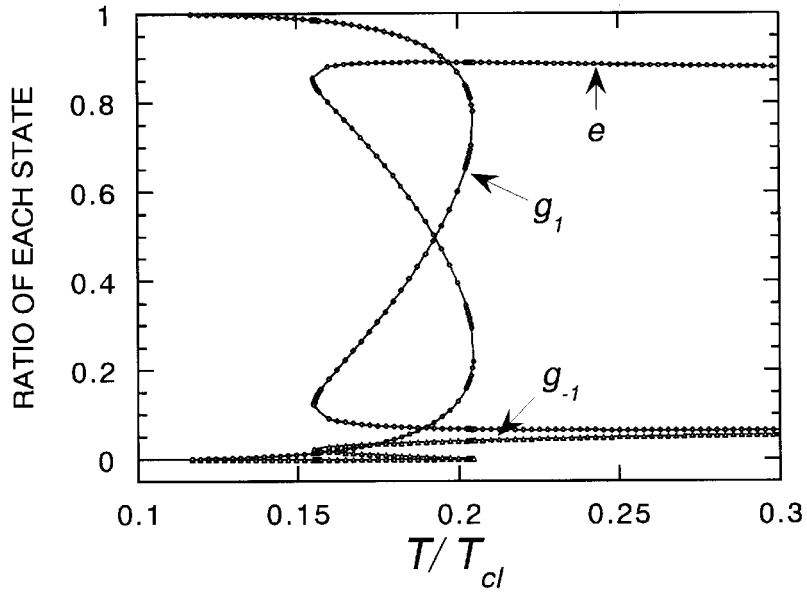

FIG. 4. Temperature dependence of the existence ratio of each state when n equals -0.8.

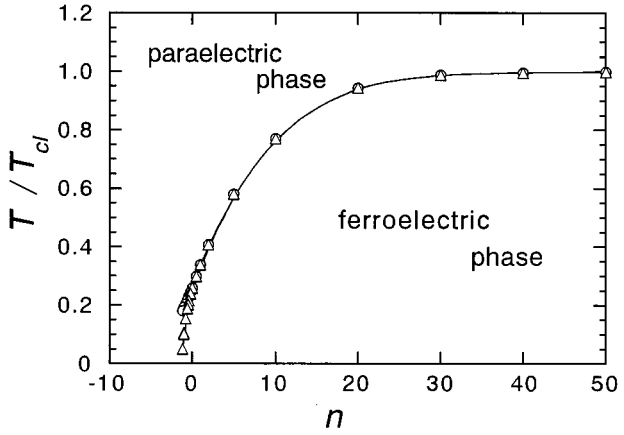

FIG. 5. Phase diagram on n-T plane when A equals 10.

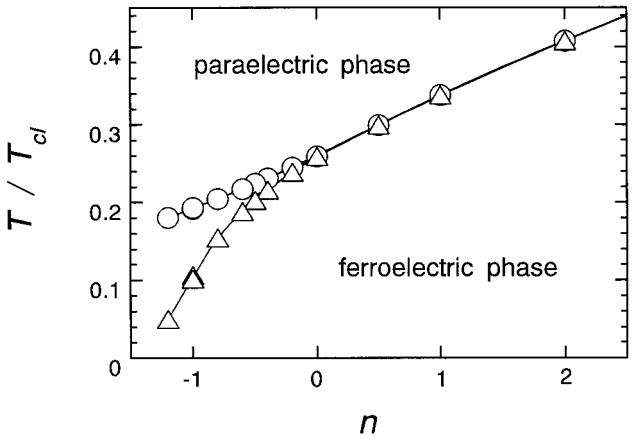

FIG. 6. Phase diagram of a magnified part of Fig. 5.

to affect the transition in the vicinity of $n=20$. In Fig. 6 we can see that the temperature hysteresis of the transition is revealed with a change in the sign of n. We believe that variation in the phase transition seen in a series of copolymers of VDF and TrFE occurs in the region shown in Fig. 6 [3]. Therefore, the transition occurs in the condition far from the critical condition of the Ising model.

In Fig. 7, the transition temperatures are shown as functions of A for various values of n. Each trajectory splits into two lines, which means two transition temperatures T_{th} and T_{tl}. The splitting temperature is a critical temperature at which the second order phase transition occurs. The figure shows the critical temperature $0.26T_{cI}$ is independent of both n and A.

Figure 8 shows a transition map on a plane in which n and A are taken as two parameters. The straight line is a critical line that divides the first order phase transition region and the diffuse transition region. On the critical line, the second order phase transition is occurring. Considering the facts that W of a 52-48 (VDF mol %–TrFE mol %) copolymer is positive and that of 73-27 is negative and, furthermore, the former does not exhibit the temperature hysteresis but the latter does, we can assume that the change in the situation in this copolymer takes place in the neighborhood of $A=10$ in this model. Figure 8 shows that if A becomes much larger or smaller than 10, the character of the phase transition varies without a change in the sign of W.

VI. CRITICAL PHENOMENA

Here, we consider why T_c is independent of n and A. When the intramolecular interaction W approaches positive infinity the behavior of our model approaches the Ising model because the state e cannot be excited across an infinite energy. Then temperatures are scaled as

$$\frac{kT}{V}=T^{*}. \tag{21}$$

At the critical temperature T_{cI} in the Ising model, we have

$$\frac{kT_{cI}}{V}=T_{cI}^{*}, \tag{22}$$

where T_{cI}^{*} is 4.93 in the Bethe approximation [20]. The existence of an excited conformation makes the first order

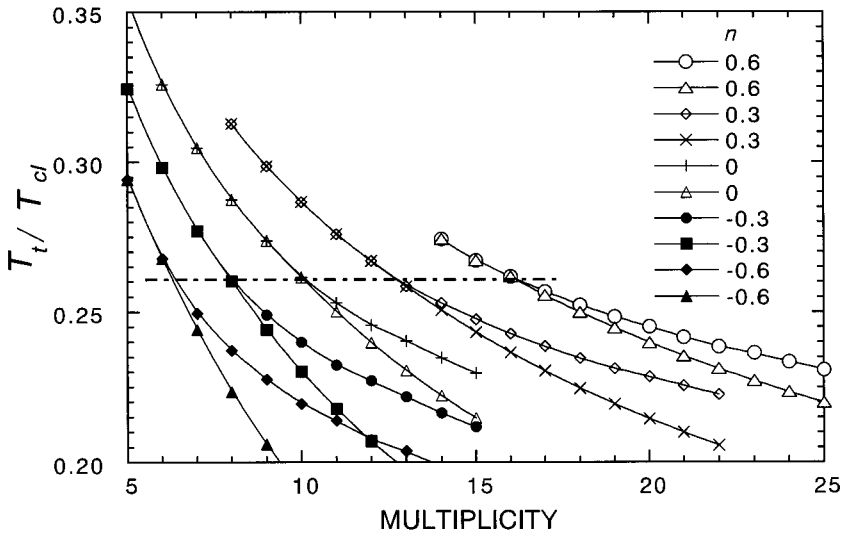

FIG. 7. Dependence of the transition temperature for the system with various values of n on the multiplicity of the excited state. The dotted line at $T_t=0.26T_c$ corresponds to the critical temperature, at which the phase transition with various n changes from the diffuse transition to the first order phase transition.

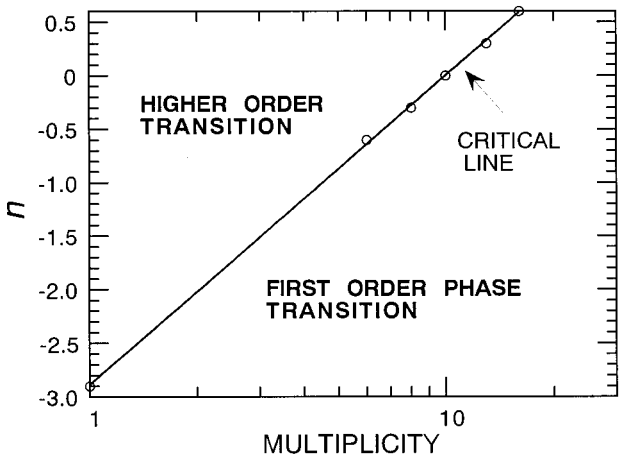

FIG. 8. Transition map on n-ln A space. Open circles show the critical temperatures calculated by the Bethe approximation. The solid line shows the critical line that is derived from those plots.

phase transition and the broad transition below T_{cI}^* and furthermore makes the new critical temperature T_c^* for this model far below T_{cI}^*. We can presume from the result in Fig. 7 that this T_c^* is also constant independent of n and A. Here, we consider what it means.

The partition function of this model is the combination of $\exp(-V/kT)$ and $A\exp(-W/kT)$. The number of variables controlling the system is reduced to 2 from 4 as

$$Z(T,V,W,A)=Z(T^*,A,W)=Z(T^*,f\ ), \tag{23}$$

where $f\equiv A\exp(-W/kT)$. The behavior of this model, whether the phase transition is thermodynamically of first or higher order, is determined by the value of f. Therefore, we assume

$$A_c\ \exp\left(-\frac{n_c}{T_c^*}\right)=C, \tag{24}$$

where C is a constant and A_c and n_c stand for A and n at the critical point. Thus we have

$$n_c=T_c^*(\ln A_c-\ln C). \tag{25}$$

When the transition map is depicted on the n-ln A space, the slope of the critical line gives us the critical temperature of the model.

From Eq. (25) and the slope of the straight line in Fig. 8, we have $T_c^*=1.28$. Since $T_{cI}^*=4.93$, we have

$$\frac{T_c^*}{T_{cI}^*}=\frac{1.28}{4.93}=0.26. \tag{26}$$

This value agrees well with the value obtained in Fig. 7. So we conclude that Eq. (24) is the condition for the corresponding state giving the same critical temperature for various combinations of n and A. The critical temperature equals $0.26T_{cI}^*$, independent of the values of A, V, and n. Furthermore, C becomes about 10.

VII. SMEARING OUT EFFECT

A smearing out effect in polymer crystals has been proposed by Peterlin *et al.* [21–23]. This effect teaches us that the depth of the potential pocket catching an atom in polymer crystals becomes shallower with increasing temperature because of thermal excitation of low frequency vibrational mode with rather large amplitude. Although this effect should be expected also in another crystal except polymer crystals, the effect is supposed to be negligibly small. In the case of a polymer crystal, however, even if an atom deviates from its lattice point by an order of unit cell length, the atom is not always impossible to recover. Such a large amplitude vibration smears out a potential localized at other atoms. Therefore, we cannot neglect this effect in polymers. The smearing out effect gives us a next relation for an intermolecular interaction.

$$V=V_0\ \exp(-ST). \tag{27}$$

Then a reduced temperature is written as

$$\frac{kT}{V_0\ \exp(-ST)}=T^*. \tag{28}$$

Let us take the temperature as $\overline{T}$ in a system where the smearing out effect is taken into account. The critical temperature of the Ising model whose interaction is smeared out is written as

$$\frac{k\overline{T_{cI}}\ \exp(S\overline{T_{cI}})}{V_0}=T_{cI}^*. \tag{29}$$

Then we have

$$\overline{T_{cI}}\ \exp(S\overline{T_{cI}})=T_{cI}. \tag{30}$$

At the critical temperature of this model, we have the same relation as Eq. (24):

$$\overline{A_c}\ \exp\left[-\frac{\overline{W_c}}{k\overline{T_c}}\right]=C. \tag{31}$$

This is rewritten as

$$\overline{n_c}=\frac{k\overline{T_c}}{V_0}\ (\ln\overline{A_c}-\ln C). \tag{32}$$

Multiplying $\exp(S\overline{T_c})$ on both sides of this equation we get

$$\overline{n_c}=T_c^*e^{-S\overline{T_c}}(\ln\overline{A_c}-\ln C). \tag{33}$$

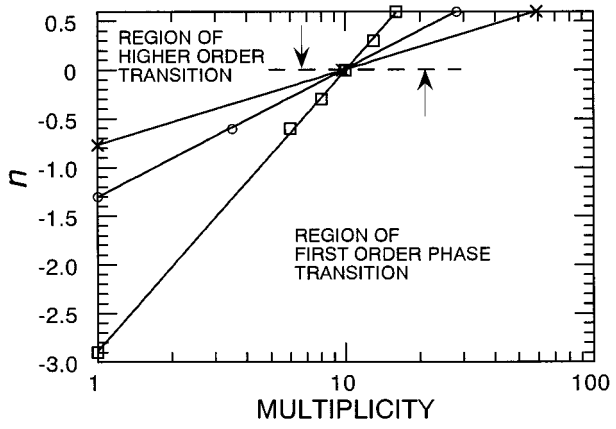

FIG. 9. Transition map. Two lines show the critical lines obtained in the model with the smearing out effect $S=0.0034$ for ○ and 0.01 for ×. The other line is the same as that in Fig. 8. The two arrows in the figure show the direction of the effect that application of hydrostatic pressure gives to the system.

Figure 9 shows a result calculated by the Bethe approximation. The two lines show the results obtained by the condition $V_0=0.8$ kcal/mol, $S=0.0034$ and 0.01. The value 0.0034 was obtained by substituting 1000, 5×10^5 dyn/cm, and 1.26 Å for N, f, and c in the following equation derived by Peterlin, which are the lamella thickness measured by the number of carbons, a force constant of a molecular chain, and a length between carbons projected onto a molecular axis, respectively:

$$\frac{V}{V_0}=\exp\left(-\frac{\pi^2}{5}\frac{NkT}{fc^2}\right). \tag{34}$$

Since the critical temperatures become 235 and 135 K for $S=0.0034$ and 0.01, respectively, we find the slope of the respective lines as 0.58 and 0.34 from Eq. (31) or (32). These results agree well with those of the numerically calculated lines. In the same manner as Eq. (26) we have

$$\frac{\overline{T_c^*}}{\overline{T_{cI}^*}}=0.26\exp[S(\overline{T_{cI}}-\overline{T_c})]. \tag{35}$$

The smearing out effect softens the slope of the critical line in the n-$\ln A$ space, as shown in Fig. 9. In the region $W<0$, the region of the first order phase transition is enlarged, but in the region $W>0$ it becomes small.

VIII. EFFECTS OF THE EXTERNAL FIELD

A. Hydrostatic pressure

Hydrostatic pressure works upon a molecular system through the intermolecular interaction. The intermolecular interaction is strengthened due to the change in the intermolecular spacing by an application of the hydrostatic pressure but the intramolecular interaction is not influenced because an interatomic length within the same molecule hardly changes because of the strength of the covalent bond. Since the absolute value of V increases when the hydrostatic pressure is applied, n shifts toward zero as shown in Fig. 9. The effect of the hydrostatic pressure upon the ferroelectric phase transition differs due to the sign of the intramolecular interaction since n goes down or goes up in the transition map according to whether the intramolecular interaction is positive or negative. In the former case where n goes down, the system strengthens its character of the first order phase transition; i.e., the temperature hysteresis increases. But in the latter case, it does the character of the diffuse transition. In the case of the VDF-TrFE copolymer, the hydrostatic pressure enlarges the hysteresis in the case $W>0$ corresponding to the 52-48 copolymer but reduces it in the case $W<0$ corresponding to 73-27 [3]. This result is supported by a preliminary experiment under high pressure [24] although we think the change in the thermal hysteresis should be studied more precisely.

B. Tensile stress

We consider a tensile stress applied to a uniaxially oriented ferroelectric VDF copolymer. In this situation, the tensile stress rather prefers a planar zigzag conformation composed of the trans bonds to the helixlike conformation made of mixing of trans and gauche bonds because the length along the molecular axis of a planar zigzag conformation is longer than that of the helixlike one. Therefore, application of the tensile stress means making a bias toward the ferroelectric state. The tensile stress makes a larger positive W value and n increases. When the phase transition of the system has the temperature hysteresis, the hysteresis decreases due to application of tensile stress.

C. Electric field

An external electric bias field usually prefers the ferroelectric state whose polarization is directed parallel to the external field to the paraelectric state. Therefore, the effect of the electric field upon the VDF copolymer is the same as that of the tensile stress.

IX. CONCLUSION

We proposed a model for the ferroelectricity of polymers that has two conformational degrees of freedom and two directional degrees of freedom for the ground state comformation and analyzed the transition behavior by the Bethe approximation. We found a critical phenomenon at $0.26T_{cI}$, which is independent of the intramolecular conformational situation of the molecular chain such as the intramolecular interaction and the multiplicity of the excited conformation. The transition becomes a first order phase transition under the condition that the transition occurs below $0.26T_{cI}$, whereas it becomes the diffuse transition under the condition that the transition occurs above $0.26T_{cI}$. This change in the transition behavior near $0.26T_{cI}$ explains the variation in the ferroelectric phase transition occurring with the change in the

VDF fraction in the copolymer. This critical temperature falls due to introduction of the smearing out effect.

Effects of the external field upon the ferroelectric phase transition were investigated. Hydrostatic pressure on the system with the negative intramolecular interaction, which means advantage of the gauche bond against the trans bond, enhanced the properties appearing in the first order phase transition. On the other hand, it enhanced the properties appearing in the diffuse transition in the case of the system with the positive intramolecular interaction.

[1] T. Furukawa, M. Date, and E. Fukada, J. Appl. Phys. **51**, 1135 (1980).
[2] M. Jimbo, T. Fukada, H. Takeda, F. Suzuki, K. Horino, K. Koyama, S. Ikeda, and Y. Wada, J. Polym. Sci. Polym. Phys. Ed. **24**, 909 (1986).
[3] K. Tashiro, K. Takano, M. Kobayashi, Y. Chatani, and H. Tadokoro, Ferroelectrics **57**, 297 (1984).
[4] T. Furukawa, Phase Transit. **18**, 143 (1989).
[5] F. J. Balta Calleja, A. Gonzalez Arche, T. Ezquerra, C. Santa Cruz, F. Batallan, B. Frick, and E. Lopez Cararos, *Advances in Polymer Science 108*, edited by H. G. Zachmann (Springer-Verlag, Berlin, 1993), p. 1.
[6] A. Lovinger, Jpn. J. Appl. Phys., Part 2 **24**, 18 (1985).
[7] H. Ohigashi and T. Hattori, Ferroelectrics **171**, 11 (1995).
[8] S. Ikeda, H. Kominami, K. Koyama, and Y. Wada, J. Appl. Phys. **62**, 3339 (1987).
[9] S. Ikeda, H. Suzuki, and S. Nagami, Jpn. J. Appl. Phys., Part 1 **31**, 1112 (1992).
[10] Y. Takahashi, Y. Nakagawa, H. Miyaji, and K. Asai, J. Polym. Sci. Part C **25**, 153 (1987).
[11] M. G. Broadhurst and G. T. Davis, Ferroelectrics **32**, 177 (1981).
[12] R. B. Olsen, J. C. Hicks, M. G. Broadhurst, and G. T. Davis, Appl. Phys. Lett. **43**, 127 (1983).
[13] A. Odajima, Ferroelectrics **57**, 159 (1984).
[14] S. Ikeda and H. Suda, Rep. Prog. Polym. Phys. Jpn. **31**, 383 (1988).
[15] S. Ikeda and H. Suda, Rep. Prog. Polym. Phys. Jpn. **32**, 331 (1989).
[16] P. R. Silva, B. V. Costa, and R. L. Moreira, Polymer **34**, 3107 (1993).
[17] B. L. Farmer, A. J. Hopfinger, and J. B. Lando, J. Appl. Phys. **43**, 4293 (1972).
[18] C. K. Purvis and P. L. Taylor, J. Appl. Phys. **54**, 1021 (1983).
[19] R. Al-Jishi and P. L. Taylor, J. Appl. Phys. **57**, 897 (1985).
[20] H. A. Bethe, Proc. R. Soc. London, Ser. A **150**, 552 (1935).
[21] A. Peterlin and E. W. Fischer, Z. Phys. **159**, 272 (1960).
[22] A. Peterlin, E. W. Fischer, and Chr. Reinhold, J. Chem. Phys. **37**, 1403 (1962).
[23] P. H. Geil, *Polymer Single Crystals* (Interscience Publishers, New York, 1963), p. 402.
[24] K. Matsushige, Phase Transit. **18**, 247 (1989).